SCIENTIFIC REPORTS

OPEN

SUBJECT AREAS:
QUANTUM MECHANICS
STATISTICAL PHYSICS
PHASE TRANSITIONS AND CRITICAL PHENOMENA

Received
13 February 2014

Accepted
19 May 2014

Published
6 June 2014

Correspondence and requests for materials should be addressed to R.-B.L. (rbliu@phy.cuhk.edu.hk)

Phase transitions in the complex plane of physical parameters

Bo-Bo Wei, Shao-Wen Chen, Hoi-Chun Po & Ren-Bao Liu

Department of Physics, Centre for Quantum Coherence, and Institute of Theoretical Physics, The Chinese University of Hong Kong, Shatin, New Territories, Hong Kong, China.

At low temperature, a thermodynamic system undergoes a phase transition when a physical parameter passes through a singularity point of the free energy. This corresponds to the formation of a new order. At high temperature, thermal fluctuations destroy the order. Correspondingly, the free energy is a smooth function of the physical parameter and singularities only occur at complex values of the parameter. Since a complex valued parameter is unphysical, no phase transitions are expected when the physical parameter is varied. Here we show that the quantum evolution of a system, initially in thermal equilibrium and driven by a designed interaction, is equivalent to the partition function of a complex parameter. Therefore, we can access the complex singularity points of thermodynamic functions and observe phase transitions even at high temperature. We further show that such phase transitions in the complex plane are related to topological properties of the renormalization group flows of the complex parameters. This result makes it possible to study thermodynamics in the complex plane of physical parameters.

The physical properties of a many-body system in the thermodynamic equilibrium are fully determined by the partition function $Z(\beta,\lambda_1,\lambda_2,\ldots,\lambda_k)$, which is a function of the coupling parameters $\{\lambda_k\}$ of the system and the temperature T (or the inverse temperature $\beta \equiv 1/T$). The partition function is the summation of the Boltzmann factor $e^{-\beta H(\lambda_1,\lambda_2,\ldots,\lambda_K)}$ over all energy eigen states, i.e., $Z=\mathrm{Tr}\left[e^{-\beta H(\lambda_1,\lambda_2,\ldots,\lambda_K)}\right]$, where the Hamiltonian $H=\sum_k \lambda_k H_k$ is characterized by a set of coupling parameters $\{\lambda_k\}$ (e.g., in spin models the magnetic field $h=\lambda_1$, the nearest neighbor coupling $J=\lambda_2$, and the next nearest neighbor coupling $J'=\lambda_3$, etc.). The normalized Boltzmann factor $Z^{-1}\exp(-\beta H)$ is the probability that the system is in a state with energy H.

At a sufficiently low temperature ($\beta > |\lambda_k|^{-1}$), the many-body system may have different orders (phases) in different parameter ranges and therefore phase transitions may occur when these parameters are varied (see Fig. 1a). Phase transitions correspond to non-analytic or singularity points of the free energy F (which is related to the partition function by $F=-\beta^{-1}\ln Z$). For a finite-size system, the partition function is always positive and hence the free energy always analytic for real physical parameters. The partition function can be zero for complex temperature or complex coupling parameters (see Fig. 1b & 1c). Such is the case for Lee-Yang zeros[1,2] in the complex plane of magnetic field for a spin lattice and Fisher zeros[3] in the complex plane of temperature. At a sufficiently low temperature and in the thermodynamic limit (where the number of particles in the system approaches infinity), the zeros of the partition function can approach to real axes of the coupling parameters, and, hence, phase transitions can occur[1,2] (see Fig. 1c). At high temperature, the free energy would be non-analytic only for complex values of temperature and coupling parameters[3–5] (see Fig. 1b). Therefore, no phase transitions would occur (see Fig. 1a). Physically, this is because, at high temperatures, thermal fluctuations destroy all possible orders and prevents the phase transitions. Phase transitions at high temperatures would be possible if one could access complex parameters, which, however, are generally regarded as unphysical.

Here we present a systematic approach to the complexification of an arbitrary physical parameter, using a quantum evolution that involves a complex phase factor. There are two fundamental laws of physics that involve probabilistic distributions. One is the Boltzmann distribution $Z^{-1}\exp(-\beta H)$, the *probability* of a system being in a state with energy H at inverse temperature β. The other is the Schrödinger equation that gives $\exp(-itH)$, the *probability amplitude* of a system being in a state with energy H at time t. The unit imaginary number $i\equiv\sqrt{-1}$ is associated with the time in quantum evolution. Thus a time-dependent measurement of the system

$$L(t)=Z^{-1}\mathrm{Tr}[\exp(-\beta H-itH_I)] \quad (1)$$

has the form of a partition function with an imaginary coupling parameter it/β. By choosing H_I to be the k-th component of $H=\sum_k \lambda_k H_k$, i.e., $H_I=H_k$, the k-th coupling parameter is analytically continued to the complex

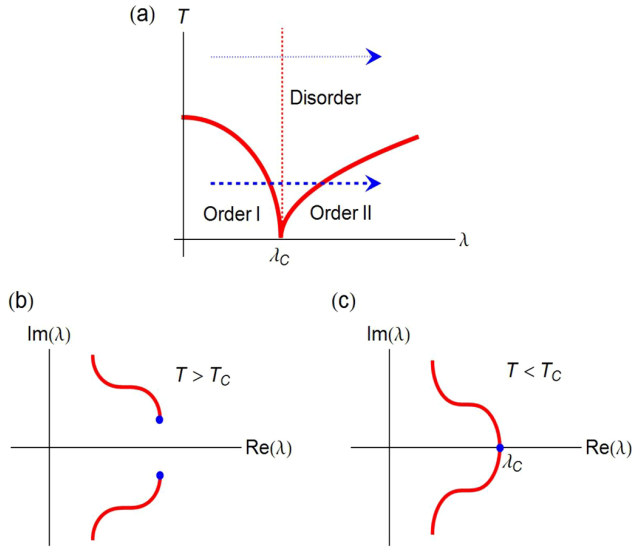

Figure 1 | Phase transitions and zeros of a partition function in the complex plane of a physical parameter. (a). The schematic phase diagram of a general many-body system. At low temperature, the system has two ordered phases, I and II, separated by a critical parameter λ_c. At high temperature, the system is in the disordered phase. When we tune the control parameter at low temperatures (as indicated by blue dashed arrow) we cross two phase boundaries (indicated by solid-red lines) and therefore experience two phase transitions. Conversely at high temperature sweeping the parameter in the same range (blue dotted arrow) would not cause a phase transition. (b). The schematic distribution of zeros of the partition function in the complex plane of the parameter for temperature T above the critical point T_c. The two blue points mark the edge singularities. (c). The same as (b) but for the temperature below the critical point ($T < T_c$). The singularity edges approach to the real axis in the thermodynamic limit.

plane via $\lambda_k \rightarrow \lambda_k + it/\beta$. One can also realize complexification of the inverse temperature ($\beta \rightarrow \beta + it$) by choosing $H_I = H$. Such a time-domain measurement, as will be discussed later in this paper, is experimentally realizable, though non-trivial in general. The time-domain measurement in equation (1) is fully determined by the *equilibrium-state* partition function of the system. The measurement result will be zero when a zero of the partition function in the complex plane is encountered[6]. Lee-Yang zeoros have been recently observed via such measurement[7]. Furthermore, critical times may exist corresponding to the singularity points in the complex plane, as indicated by recent studies of central spin decoherence caused by an Ising bath[6] and evolution of a quantum spin model[8]. The measurement in equation (1) provides a systematic approach to accessing different types of zeros in the complex plane for the partition function, such as Lee-Yang zeros[1,2] by choosing $H_I = \sum_j S_j^z$ for a system of spins $\{\mathbf{S}_j\}$, Fisher zeros[3] by choosing $H_I = H$[8], and other types of zeros (yet unnamed) by choosing $H_I = \sum S_j^x S_{j+1}^x$, $H_I = \sum \mathbf{S}_j \cdot \mathbf{S}_{j+1}$, etc. More importantly, by complexification of a physical parameter, we have a way to access the singularity points in the complex plane and to reveal phase transitions at high temperature ($\beta^{-1} \gg \{|\lambda_k|\}$) via time-domain measurement. The high-temperature phase transitions are also inferred from a recent finding that quantum criticality can emerge at high temperatures by long-time quantum evolution[9]. Note that the phase transitions studied in this paper are not the time-domain or dynamical phase transitions studied in Refs. 6 & 8. Instead, they occur between different parameter regimes, signified by the qualitative changes of time-domain measurement.

High-temperature magnetic phase transitions. Spin systems can have ferromagnetic (FM) or antiferromagnetic (AFM) orders at low temperatures, corresponding to positive or negative coupling (J) between the spins, respectively. Thus an FM-AFM transition would occur if the coupling J varies from positive to negative. At high temperatures, thermal fluctuations destroy the magnetic order and hence no phase transition is expected with changing J. Here we study the Ising spin model to demonstrate the FM-AFM transition in the complex plane of the parameter J. The Hamiltonian for the general Ising model is

$$H = -\sum_{i,j} J_{ij}\sigma_i\sigma_j - h\sum_j \sigma_j, \qquad (2)$$

where J_{ij} is the coupling between spins σ_i and σ_j, h is the magnetic field, and the spins σ_j take values ± 1. At low temperatures, when the coupling changes from positive to negative, the Ising model presents a phase transition from the FM order to the AFM order at zero field. Correspondingly, the Lee-Yang zeros in the complex plane of scaled magnetic field $z \equiv \exp(2\beta h)$ exhibit different distributions. Note that the distinct features of Lee-Yang zeros distribution in the complex plane persist even at high temperatures ($T \gg |J_{ij}|$).

To be specific, we study the one-dimensional (1D) Ising model with nearest-neighbor coupling J, which can be exactly solved through the transfer matrix method[10–12] (see Supplementary Information). There is no finite temperature phase transition in the 1D Ising model. The Lee-Yang zeros of the 1D Ising model of N spins have been exactly calculated[2]. We plot the distribution of Lee-Yang zeros in Fig. 2a. For AFM coupling ($J < 0$), all the zeros lie on the negative real axis (indicated by the red surface) (Fig. 2a). While for the FM coupling ($J > 0$), the zeros are distributed on an arc of the unit circle (indicated by the blue surface) (Fig. 2a). At the transition point ($J = 0$), all the Lee-Yang zeros are degenerate at $z_n = -1$ (indicated by the green solid ball).

To observe the Lee-Yang zeros and the critical behaviors in the complex plane[4,5], we study the time-domain measurement in equation (1) by choosing $H_I = \sum_j \sigma_j$ and analytically continuing the magnetic field to the complex plane $h \rightarrow h + it/\beta$. In this case, the time-domain measurement corresponds to decoherence of a quantum probe spin coupled to the Ising model[6,7] (see physical realizations). Figs. 2b–e plot the time-domain measurement calculated for different coupling parameters J at fixed inverse temperature $\beta = 1$ (which is a high temperature case for the 1D Ising model, since the critical temperature of this model is zero). For AFM coupling $J = -1$, the time-domain measurement has no zeros (Fig. 2b) and it is a smooth function of time. On the contrary, for the FM coupling $J = 1$, the time-domain measurement shows a number of zeros (Fig. 2c), which have a one-to-one correspondence to the Lee-Yang zeros[6]. Approaching the thermodynamic limit, the Yang-Lee edge singularities (the starting and ending Lee-Yang zeros along the arcs)[4,5] lead to critical times in the time-domain observation[6]. To demonstrate this, we perform a finite size scaling analysis on the time-domain measurement and show the scaled results $|L(t)|^{1/N}$ in Figs. 2d & 2e. The profiles of the time-domain measurement in the FM and AFM regions are qualitatively different. For AFM coupling, the scaled measurement is a smooth function of time (Fig. 2d). While for FM coupling, the scaled measurement presents sudden changes at critical times corresponding to the Yang-Lee edge singularities (Fig. 2e). The profiles of the time-domain measurement in the FM and AFM regions cannot be smoothly transformed into each other, which is the signature of the onset of a high-temperature phase transition.

We further study the high-temperature AFM-FM phase transition in the time-domain measurement for a two-dimensional (2D) Ising model. Specifically, we consider a 2D Ising model in a square lattice with nearest neighbor coupling J. This model under zero field is exactly solvable[11,12] and has a finite-temperature phase transition at $\beta_C \approx 0.44/|J|$. Fig. 3 shows the time-domain measurement in the 2D

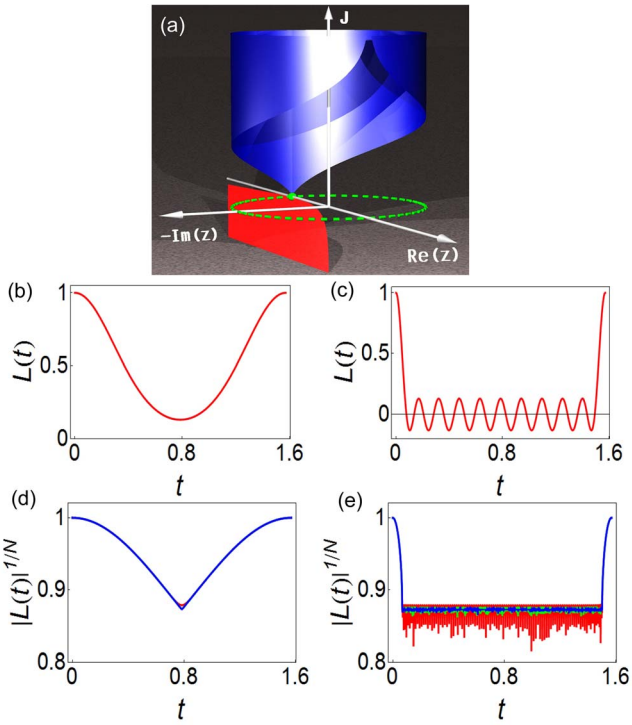

Figure 2 | High-temperature AFM-FM phase transitions revealed by time-domain observation. (a). Schematic 3D plot of the Lee-Yang zeros in the 1D Ising model. For $J > 0$, the Lee-Yang zeros are distributed on an arc of the unit circle with two edge singularity points determined by the coupling strength (blue surface). As the coupling strength decreases the arcs shrink and finally the singularity edges merge to a point at $z = -1$ for $J = 0$ (indicated by the green solid ball). For $J < 0$, the Lee-Yang zeros lie on the negative real axis (red surface). (b). The time-domain measurement as a function of time for 1D Ising model with $N = 20$ spins at $\beta = 1$ and $J = -1$ (AFM). (c). The same as (b) but for $J = 1$ (FM). (d). Finite size scaling of the time-domain measurement in the 1D Ising model at $\beta = 1$ and $J = -1$ (AFM), the red line is for $N = 100$ spins, green line for $N = 500$ and blue line for $N = 1000$; (e). The same as (d) but for $J = 1$ (FM).

Ising model calculated for different coupling parameters J at a fixed high temperature, $\beta = 0.3 < \beta_C$. For the AFM coupling $J = -1$, the partition function has no Lee-Yang zeros on the unit circle ($|z| \equiv |\exp(2\beta h)| = 1$)[13] and therefore the time-domain measurement has no zeros (Fig. 3a). While for the FM coupling $J = 1$, the time-domain measurement presents a number of zeros (equal to the number of spins) (Fig. 3b), corresponding to the Lee-Yang zeros along the unit circle. We do finite-size scaling analysis in Fig. 3c and Fig. 3d for AFM coupling and FM coupling, respectively. It is clear that the time-domain measurement is a smooth function of time for the AFM coupling, while it presents sudden changes at critical times corresponding to the Yang-Lee edge singularities for the FM coupling (Fig. 3d). Thus a phase transition with varying the coupling constant J occurs at a temperature higher than the critical temperature ($\beta < 0.44/|J|$).

Renormalization group theoretic analysis. The renormalization group (RG) method, a powerful tool for studying conventional phase transitions, can be applied to the phase transitions in the complex plane of physical parameters. Since the phase of any complex number is defined modulo 2π, the RG flows of complex parameters can present novel topological structures.

As an example we first consider the 1D Ising model and define the dimensionless parameters $K_0 = \beta J$ and $h_0 = \beta h$. The renormalization of the model can be exactly formulated by blocking two neighboring

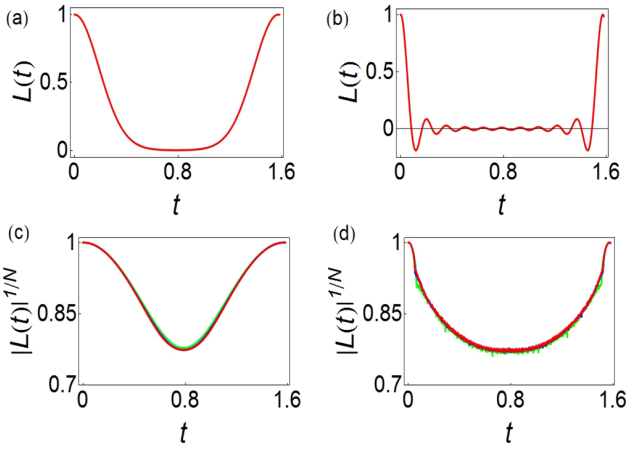

Figure 3 | High-temperature AFM-FM phase transitions of the 2D Ising spin model in a square lattice revealed by time-domain observation. a. The time-domain measurement as a function of time for the 2D Ising model in a $N = 4 \times 5$ square lattice, $\beta = 0.3$ and $J = -1$ (AFM). b. The same as (a) but for $J = 1$ (FM). c. Finite size scaling of the time-domain measurement with $\beta = 0.3$ and $J = -1$ (AFM), the green line is for $N = 4 \times 100$ spins, the blue line is for $N = 6 \times 100$ and red line for $N = 8 \times 100$. d. The same as (c) but for $J = 1$ (FM).

spins into one (Fig. 4a)[14]. By continuation of the dimensionless external field to a purely imaginary value $h_0 = i\tau_0/2$ (the physical external field is zero), the exact RG flow equations become[14]

$$\begin{cases} \tau_1(\tau_0, K_0) = \tau_0 - i \ln\left(\dfrac{\cosh(2K_0 + i\tau_0/2)}{\cosh(2K_0 - i\tau_0/2)}\right) \\ K_1(\tau_0, K_0) = \dfrac{1}{4}\ln\left(\dfrac{\cosh(4K_0) + \cos\tau_0}{1 + \cos\tau_0}\right) \end{cases}, \tag{3}$$

where the coupling K_1 remains real after renormalization. Since τ is defined modulo 2π, the parameter space can be identified with the surface of an infinitely long cylinder with unit radius. The original system corresponds to the parameter curve $K = K_0$ and $-\pi < \tau_0 \leq \pi$, and therefore its winding number ($W_\#$), defined to be the number of times the parameter curve wraps around the cylinder, is 1 (Fig. 4b).

The parameter curve is renormalized according to the RG flow equations. Since $K_1(\tau_0, K_0) = K_1(\tau_0, -K_0)$ in Eq. (3), the distinct behaviors of the FM and AFM Ising chains are encoded entirely in different RG flows of τ. This is illustrated in Figs. 4c–h. Figs. 4c, 4e & 4g show that after successive renormalization, the winding number in the FM case ($K_0 = 1/8$) becomes 2, 4, 8,.... On the contrary, the winding number in the AFM case ($K_0 = -1/8$) is zero after renormalization (Figs. 4d, 4f & 4h). The RG flow equations become trivial at the phase transition point $K_0 = 0$, which corresponds to the infinite temperature limit, and the winding number remains unchanged ($W'_\# = 1$) after the renormalization. In summary, the winding numbers for different couplings after k steps of renormalization are

$$W_\# \to W_\#^{(k)} = \begin{cases} 0 & \text{for} \quad K_0 < 0 \\ 1 & \text{for} \quad K_0 = 0 \\ 2^k & \text{for} \quad K_0 > 0 \end{cases}. \tag{4}$$

The different topologies of the RG flows demonstrate unambiguously the high-temperature phase transition with varying the coupling parameter.

We further consider the RG flows of the 2D Ising model in a square lattice. By continuation of the external field to a purely imaginary value of $h = i\tau/2$, the approximate RG flow equations read[15] (See Supplementary Information for derivation)

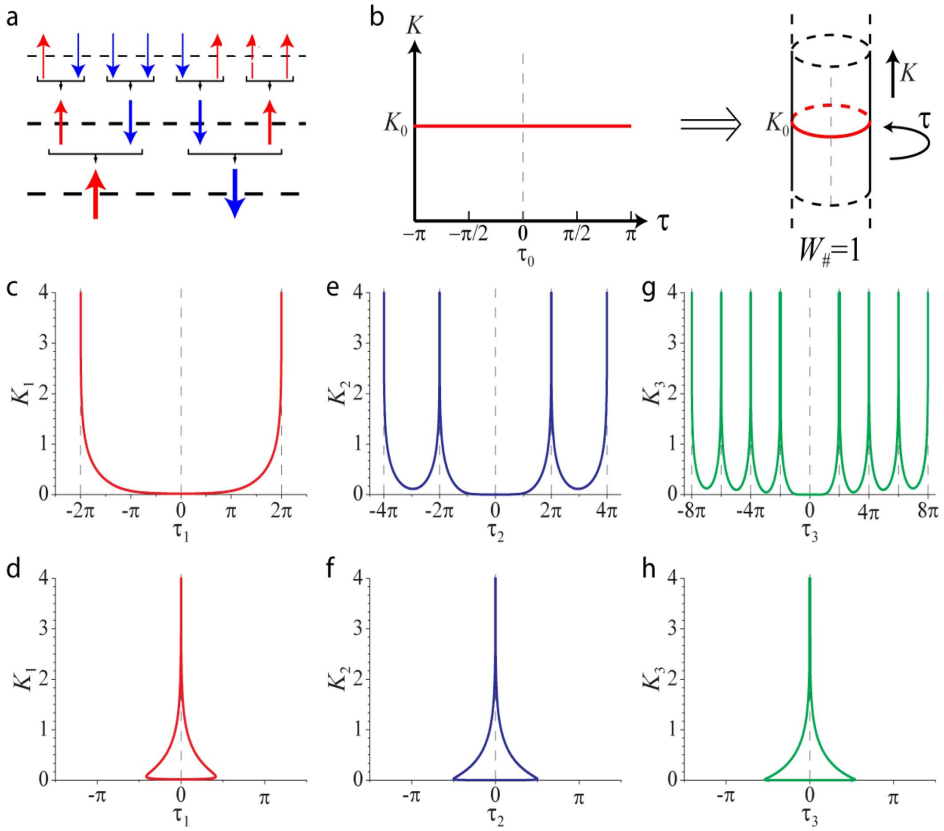

Figure 4 | Renormalized parameters of the 1D Ising model with a purely imaginary field. (a), Real-space renormalization scheme. In each renormalization step the spins on every other site are traced out, which effectively combines pairs of neighboring spins into block spins with renormalized coupling and external field. (b), The un-renormalized parameters. The spin coupling K and evolution time τ (i.e., imaginary part of the external field) form a space identical to the surface of an infinitely long cylinder. When the imaginary field τ is varied at a fixed value of $K = K_0$, the curve winds about the cylinder once and so the winding number $W_{\#} = 1$. (c–h), Under RG flow, the original curve depicted in (a) would transform differently in the different parameter regimes of K_0. (c), (e) and (g) in turn show the parameters for the FM case with $K_0 = 1/8$ after one, two, and three steps of renormalization. (d), (f) and (h) show the corresponding results for the AFM case with $K_0 = -1/8$. The vertical dashed lines indicate $\tau = 0 \bmod(2\pi)$, which are identified as the same line when represented on an infinitely long cylinder. The winding numbers can be directly inferred from the number of times the renormalized curve crosses this line.

$$\begin{cases} \tau_1(\tau_0,K_0)\approx\tau_0-\dfrac{i}{2}\ln\left(\dfrac{\cosh(4K_0+i\tau_0/2)\cosh^2(2K_0+i\tau_0/2)}{\cosh(4K_0-i\tau_0/2)\cosh^2(2K_0-i\tau_0/2)}\right) \\ K_1(\tau_0,K_0)\approx\dfrac{3}{16}\ln\left(\dfrac{\cosh(8K_0)+\cos(\tau_0)}{1+\cos(\tau_0)}\right) \end{cases}. \quad (5)$$

Fig. 5 presents the RG flows of the parameters in the FM and AFM cases. Figs. 5a, c & e present the renormalized parameters under one, two and three applications of the renormalization transformation for the FM case ($K_0 = 1/8$). Figs. 5b, d & f present the results for the AFM case ($K_0 = -1/8$). The winding numbers of the different cases after k steps of renormalization are

$$W_{\#}\to\begin{cases} [(5/2)^k] & \text{for} \quad K_0>0 \\ 1 & \text{for} \quad K_0=0, \\ [(5/2)^{k-1}/2] & \text{for} \quad K_0<0 \end{cases} \quad (6)$$

where $[x]$ is the integer part of x. The winding number of the parameters under RG reflects the different topologies intrinsic to the RG flow equations in the different parameter regimes.

Transverse-field Ising model. The models considered above are all classical models in which different components of the Hamiltonian commute. A natural question arises about whether the high-temperature phase transitions with complex parameters would exist also for quantum models. To address this question, we study the 1D transverse-field Ising model. The model contains N spin-1/2 with nearest neighbor interaction (λ_1) along the x-axis and under a transverse field (λ_2) along the z-axis, described by the Hamiltonian

$$H=\lambda_1 H_1+\lambda_2 H_2=\lambda_1\sum_{j=1}^{N}\sigma_j^x\sigma_{j+1}^x+\lambda_2\sum_{j=1}^{N}\sigma_j^z, \quad (7)$$

where $\sigma_j^{x/y/z}$ is the Pauli matrix of the j-th spin along the $x/y/z$-axis. This model is exactly solvable[16]. It has a quantum phase transition between a magnetic ordered phase for $|\lambda_1| > |\lambda_2|$ and a disordered phase for $|\lambda_1| < |\lambda_2|$ at zero temperature, but has no finite-temperature phase transition for any parameters on the real axis. By defining the dimensionless magnetic field $h = \lambda_2/\lambda_1$, the Lee-Yang zeros are determined by $\mathrm{Re}(h)^2 + \mathrm{Im}(h)^2 = 1 + [(n + 1/2)\pi/\beta]^2$, $|\mathrm{Re}(h)| \le 1$. Therefore, the zeros are located on circles and have cutoff at singularity edges $\mathrm{Re}(h) = \pm 1$, $\mathrm{Im}(h) = \pm|(n + 1/2)\pi/\beta|$ (see Fig. 6a). When the temperature approaches zero ($|\beta| \to \infty$), the Lee-Yang zeros are on the unit circle. When the temperature is high ($|\beta| \ll 1$), the radii of the circles are $\sqrt{1+|(n+1/2)\pi/\beta|^2} \gg 1$. Therefore, the zeros are distributed, approximately, along horizontal lines with interval $|\pi/\beta|$. The fact that the Lee-Yang zeros exist only in the parameter range of $|h| \le 1$ indicates that the time-domain measurement of the system would present phase

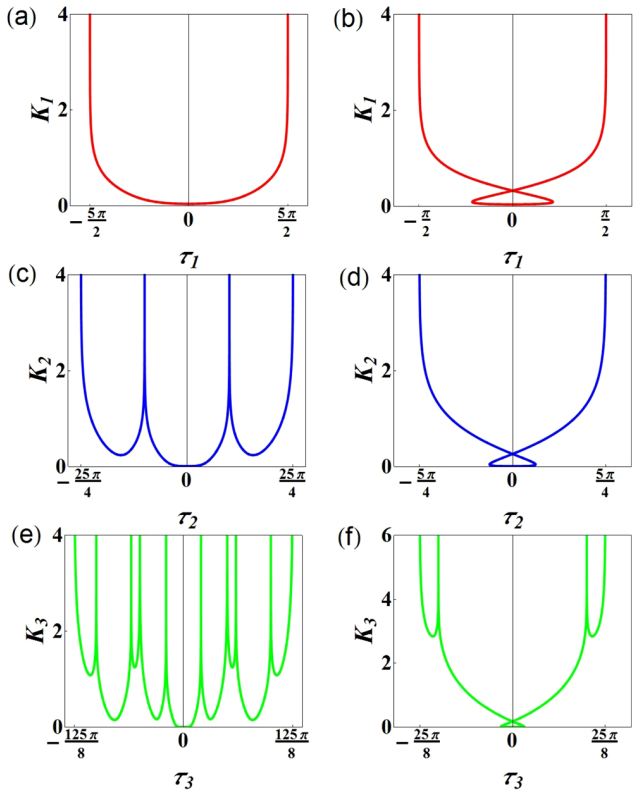

Figure 5 | Topological difference between the renormalization group flows of the FM and AFM 2D Ising models. (a), (c) & (e) present in turn the parameters (spin coupling and imaginary external field) after one, two, and three applications of the renormalization transformation in the FM case ($K_0 = 1/8$). (b), (d) & (f) are the same as (a), (c) & (e) in turn but for the AFM case ($K_0 = -1/8$). The renormalized parameters for the FM and AFM cases have different winding numbers (determined by how many periods (2π) of time the parameter curves are spanned over).

transitions between the two parameter regions, $|\lambda_2| > |\lambda_1|$ and $|\lambda_2| < |\lambda_1|$. Specifically, the time-dependent measurement can be devised as $L(t) = Z^{-1}\mathrm{Tr}[\exp(-\beta H - itH_2)]$, which is the partition function with a complex external field ($\lambda_2 \to \lambda_2 + it/\beta$). The contour plot of the time-domain measurement as a function of external field and time are presented in Fig. 6b. To demonstrate the phase transitions more clearly, we plot in Fig. 6c the time-domain measurement as a function of external field for different times. Since the zeros are bounded in the range $|h| \leq 1$ with Yang-Lee edge singularities at $\mathrm{Re}(h) = \pm 1$, $\mathrm{Im}(h) = \pm|(n + 1/2)\pi/\beta|$, the time-domain measurement has a sharp change when we tune the parameter from $|h| \leq 1$ to $|h| > 1$ at times $\mathrm{Im}(h) = \pm|(n + 1/2)\pi/\beta|$ (see Fig. 6c).

Physical realization. The time-domain measurement in equation (1) resembles the Loschmidt echo[17,18], or equivalently, decoherence of a central spin coupled to the system. Thus we may implement the time-domain measurement by coupling the system to a central spin through the probe-system interaction $|\uparrow\rangle\langle\uparrow|\otimes H_\uparrow(t) + |\downarrow\rangle\langle\downarrow|\otimes H_\downarrow(t)$ ($S_z \equiv |\uparrow\rangle\langle\uparrow| - |\downarrow\rangle\langle\downarrow|$) and measuring the central spin coherence. Essentially, the coherence of the probe spin is a complex phase factor associated with a real Boltzmann probability for each state of the system. Therefore the probe spin coherence measurement amounts to continuation of a physical parameter to the complex plane. If we initialize the central spin in a superposition state $|\uparrow\rangle + |\downarrow\rangle$ and the system in a thermal equilibrium state described by the canonical density matrix, $\rho = Z^{-1}\mathrm{Tr}[\exp(-\beta H)]$, the probe spin coherence is

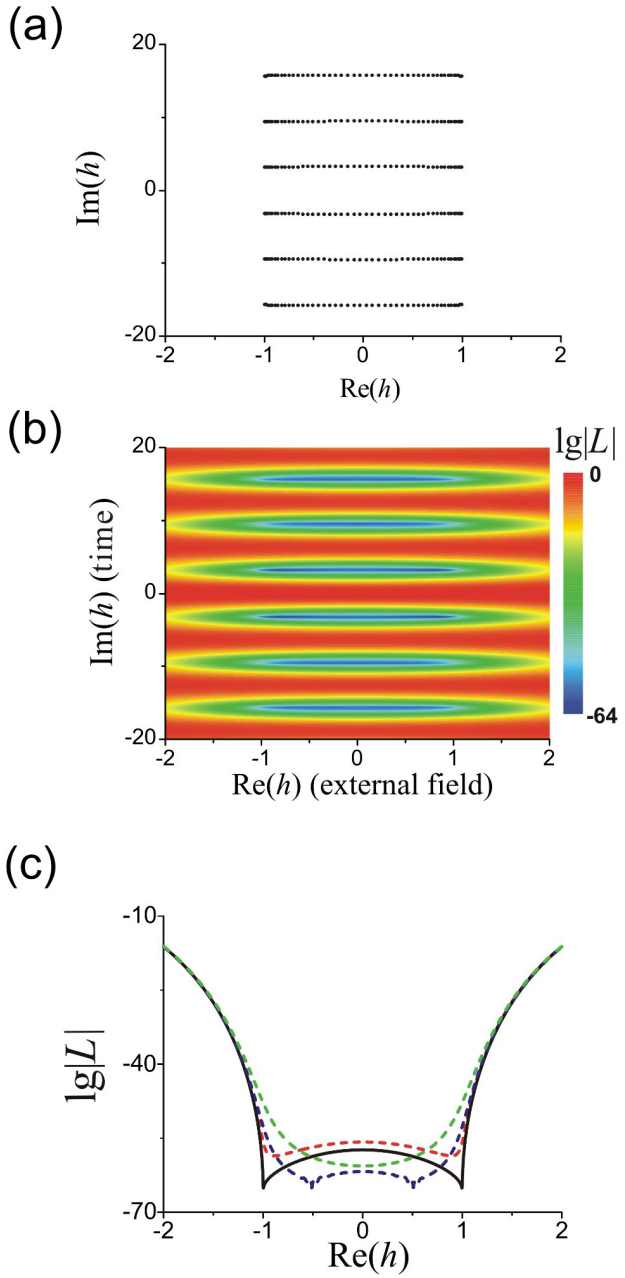

Figure 6 | Finite-temperature phase transitions of a transverse field Ising spin chain revealed by time-domain observation. The one-dimensional model contains 100 spins. The temperature is such that $\beta = 0.5$. (a). Lee-Yang zeros in the complex plane of the external field. (b). Contour plot of the time-domain measurement, $\lg|L|$, as a function of the external field $\mathrm{Re}(h)$ and the time $\mathrm{Im}(h)$. (c). $\lg|L|$ plotted as functions of the external field $\mathrm{Re}(h)$ for different times $\mathrm{Im}(h) = 3.10$ (red-dashed line), 3.14 (black-solid line), 3.26 (blue-dashed line) and 3.35 (green-dashed line). The phase transitions at $\mathrm{Re}(h) = \pm 1$ are observed.

$$\langle S_+\rangle = \langle S_x\rangle + i\langle S_y\rangle = \mathrm{Tr}\left[e^{-\beta H}e^{i(H+H_\uparrow)t}e^{-i(H+H_\downarrow)t}\right]/\mathrm{Tr}\left[e^{-\beta H}\right]. \quad (8)$$

If $[H_I, H] = 0$, the time-domain measurement $L(t) = Z^{-1}\mathrm{Tr}[\exp(-\beta H)\exp(-iH_I t)]$, which is equal to the probe spin coherence with a probe-bath coupling $H_{SB} = S_z \otimes H_I$, i.e., $H_\uparrow = -H_\downarrow = H_I/2$. Or if $[H_I, H] \neq 0$ but $[[H_I, H], H] = [[H_I, H], H_I] = 0$, the time-domain measurement can also be factored as $L(t) = Z^{-1}\mathrm{Tr}[\exp(-\beta H)\exp(-iH_I t)]$ (See Supplementary Information for details) and can be implemented by the probe spin coherence with

a modified probe-bath coupling $H_\downarrow = H_I/2 - H$ & $H_\uparrow = -H_I/2 - H$. If $[H,H_I] = isH_I$, the time-domain measurement can be written as $L(t) = Z^{-1}\mathrm{Tr}[\exp(-it \sin(s)H_I/s)\exp(-\beta H)]$ (See Supplementary Information for details), which can be implemented by probe spin decoherence with a probe-bath coupling $H_\downarrow = \sin(s)H_I/2s - H$ & $H_\uparrow = -\sin(s)H_I/2s - H$. In the general case, the time-domain measurement in equation (1) can be written as $L(t) = Z^{-1}\mathrm{Tr}[e^{-\beta H'} e^{-itH'_I}]$, with $e^{-2\beta H'} \equiv T\exp\left(-\frac{\beta}{2}\int_{-1}^{1}\tilde{H}(u)du\right)\bar{T}\exp\left(-\frac{\beta}{2}\int_{-1}^{1}\tilde{H}(u)du\right)$, $\exp(-itH'_I) \equiv \exp(\beta H')\exp(-\beta H - itH_I)$ and $\tilde{H}(u) \equiv \exp(iutH_I/2)H\exp(-iutH_I/2)$, where T and $\bar{T}$ are the time-ordering and anti-ordering operators, respectively. If one initializes the bath in a canonical state $\rho = \exp(-\beta H')/\mathrm{Tr}[\exp(-\beta H')]$, the time-domain measurement can be implemented by probe spin decoherence with probe-bath coupling $H_\downarrow = H'_I/2 - H'$ & $H_\uparrow = -H'/2 - H'$, up to a normalization factor (see Supplementary Information for details). The physical realization of the modified Hamiltonians H' and H'_I is non-trivial.

Note that the time-domain measurement in equation (1) is similar to the measurement of the characteristic function of the work distribution in a quantum quench[19-21], which plays a central role in the fluctuation relations in non-equilibrium thermodynamics[22-26]. The probe spin decoherence realization of the time-domain measurement can also be related to the quench dynamics where the evolution of the system can be controlled under different Hamiltonians for different periods of time[27].

Summary. We have shown that the quantum evolution of a system originally in thermodynamic equilibrium is equivalent to the partition function of the system with a complex parameter. By choosing different forms of coupling we have a systematic way to realize the continuation of an arbitrary physical parameter to the complex plane. The time-domain measurement allows us to study a variety of zeros of the partition function. More importantly, we can access the singularity points of thermodynamic functions in the complex plane of physical parameters and therefore observe phase transitions at high temperatures. The physical realization of the time-domain measurement may be nontrivial but in principle it can be implemented by probe spin decoherence or quantum quench experiments. This discovery makes it possible to study thermodynamics in the complex plane of physical parameters.

Methods

The 1D Ising spin model was exactly diagonalized by the transfer matrix method[10,11]. The evaluation of the partition function after the transformation becomes a trivial problem of diagonalization of a 2×2 matrix. The probe spin coherence (which has been formulated in terms of partition functions[6]) was similarly calculated. Similarly, by applying the transfer matrix method, the 2D Ising model without magnetic field was mapped to a 1D Ising model with a transverse field[10,11]. For a 2D Ising model in a finite magnetic field, it was mapped by the transfer matrix method to a 1D Ising model with both longitudinal field and transverse field[11], which was then numerically diagonalized. Therefore, the partition function and hence the probe spin coherence for the 2D Ising model in finite magnetic field were obtained. We derived the exact RG equations of the 1D Ising model and approximate RG equations for the 2D Ising model in square lattice for real parameters[14,15]. By analytic continuation we obtained the RG equations in the complex plane of the physical parameters and analyzed the RG flows of the complex parameters. The 1D Ising model with a transverse magnetic field was exactly solved[16] and the partition function and time-domain measurement were then calculated.

Full methods are included in the Supplementary Information.

1. Yang, C. N. & Lee, T. D. Statistical theory of equations of state and phase transitions. I. Theory of condensation. *Phys. Rev.* **87**, 404–409 (1952).
2. Lee, T. D. & Yang, C. N. Statistical theory of equations of state and phase transitions. II. Lattice gas and Ising model. *Phys. Rev.* **87**, 410–419 (1952).
3. Fisher, M. E. *Lectures in Theoretical Physics* [Brittin W. E.] (University of Colorado Press, Boulder, 1965).
4. Kortman, P. J. & Griffiths, R. B. Density of zeros on the Lee-Yang circle for two Ising ferromagnets. *Phys. Rev. Lett.* **27**, 1439 (1971).
5. Fisher, M. E. Yang-Lee edge singularity and φ3 theory. *Phys. Rev. Lett.* **40**, 1610 (1978).
6. Wei, B. B. & Liu, R. B. Lee-Yang zeros and critical times in decoherence of a probe spin coupled to a bath. *Phys. Rev. Lett.* **109**, 185701 (2012).
7. Peng, X. H. *et al.* Observation of Lee-Yang zeros. *arxiv:1403. 5383*(2014).
8. Heyl, M., Polkovnikov, A. & Kehrein S. Dynamical Quantum phase transitions in the transverse-field Ising model. *Phys. Rev. Lett.* **110**, 135704 (2013).
9. Chen, S. W., Jiang, Z. F. & Liu, R. B. Quantum criticality at high temperature revealed by spin echo. *New J. Phys.* **15**, 043032 (2013).
10. Kramers, H. A. & Wannier, G. H. Statistics of the two-dimensional Ferromagnet. Part I. *Phys. Rev.* **60**, 252 (1941).
11. Schultz, T. D., Mattis, D. C. & Lieb, E. H. Two-dimensional Ising model as a soluble problem of many fermions. *Rev. Mod. Phys.* **36**, 856 (1964).
12. Onsager, L. Crystal statistics. I. A Two-dimensional model with an order-disorder transition. *Phys. Rev.* **65**, 117 (1944).
13. Kim, S. Y. Density of Lee-Yang zeros and Yang-Lee edge singularity in the antiferromagnetic Ising model. *Nucl. Phys. B.* **705**, 504 (2005).
14. Pathria, R. K. *Statistical Mechanics, 2nd Ed.* (Elsevier, Oxford, 1996).
15. Maris, H. J. & Kadanoff, L. P. Teaching the renormalization group. *Am. J. Phys.* **46**, 652 (1978).
16. Sachdev, S. *Quantum Phase Transitions* (Cambridge University Press, New York, 1999).
17. Quan, H. T. *et al.* Decay of Loschmidt echo enhanced by quantum criticality. *Phys. Rev. Lett.* **96**, 140604 (2006).
18. Zhang, J., Peng, X., Rajendran, N. & Suter, D. Detection of quantum critical points by a probe qubit. *Phys. Rev. Lett.* **100**, 100501 (2008).
19. Dorner, R. *et al.* Extracting quantum work statistics and fluctuation theorems by single-qubit interferometry. *Phys. Rev. Lett.* **110**, 230601 (2013).
20. Mazzola, L., Chiara, G. D. & Paternostro, M. Measuring the characteristic function of the work distribution. *Phys. Rev. Lett.* **110**, 230602 (2013).
21. Batalhão, T. *et al.* Experimental reconstruction of work distribution and verification of fluctuation relations at the full quantum level. *arxiv, 1308.3241* (2013).
22. Campisi, M., Hanggi, P. & Talkner, P. Quantum fluctuation relations: Foundations and applications. *Rev. Mod. Phys.* **83**, 771 (2011).
23. Quan, H. T., Liu, Y. X., Sun, C. P. & Nori, F. Quantum thermodynamic cycles and quantum heat engines. *Phys. Rev. E* **76**, 031105 (2007).
24. Maruyama, K., Nori, F. & Vedral, V. The physics of Maxwell's demon and information. *Rev. Mod. Phys.* **81**, 1 (2009).
25. Zhang, W., Sun, C. P. & Nori, F. Equivalence condition for the canonical and microcanonical ensembles in coupled spin systems. *Phys. Rev. E* **82**, 041127 (2010).
26. Huang, J. F. *et al.* Quantum statistics of the collective excitations of an atomic ensemble inside a cavity. *Phys. Rev. A* **85**, 023801 (2012).
27. Polkovnikov, A., Sengupta, K., Silva, A. & Vengalattore, M. *Colloquium*: Nonequilibrium dynamics of closed interacting quantum systems. *Rev. Mod. Phys.* **83**, 863 (2011).

Acknowledgments

We thank Dr. J. A. Crosse for improving the English of our paper. This work was supported by Hong Kong Research Grants Council - General Research Fund Project 401413, The Chinese University of Hong Kong Focused Investments Scheme, and Hong Kong Research Grants Council - Collaborative Research Fund Project HKU10/CRF/08.

Author contributions

R.B.L. conceived the idea, designed project, formulated the theory, and supervised the project. B.B.W. studied magnetic phase transitions in the Ising models and calculated the RG flows of the 2D Ising model. H.C.P. discovered the topological features of the RG flows of the 1D model. S.W. studied the transverse-field Ising model. B.B.W. & R.B.L. wrote the manuscript. All authors discussed the results and the manuscript.

Additional information

Supplementary information accompanies this paper at http://www.nature.com/scientificreports

Competing financial interests: The authors declare no competing financial interests.

How to cite this article: Wei, B.-B., Chen, S.-W., Po, H.-C. & Liu, R.-B. Phase transitions in the complex plane of physical parameters. *Sci. Rep.* **4**, 5202; DOI:10.1038/srep05202 (2014).

This work is licensed under a Creative Commons Attribution-NonCommercial-ShareAlike 3.0 Unported License. The images in this article are included in the article's Creative Commons license, unless indicated otherwise in the image credit; if the image is not included under the Creative Commons license, users will need to obtain permission from the license holder in order to reproduce the image. To view a copy of this license, visit http://creativecommons.org/licenses/by-nc-sa/3.0/